Journal of Structural Geology, Vol. 11, No. 3, pp. 285 to 294, 1989
Printed in Great Britain

0191-8141/89 $03.00 + 0.00

Late Cenozoic stress field and fracturing in the Iberian Chain and Ebro Basin (Spain)

JOSÉ L. SIMÓN-GÓMEZ

Departamento de Ciencias de la Tierra, Universidad de Zaragoza, 50009 Zaragoza, Spain

(*Received* 12 *October* 1987; *accepted in revised form* 18 *August* 1988)

Abstract—Detailed study of mesoscopic faults and joints affecting Neogene and Pleistocene deposits in the Iberian Chain and the Ebro Basin, involving statistical study of fracture directions and palaeostress analysis from striated fault planes, together with analysis of macrostructures, suggest a complex late Cenozoic stress field in which both primary and secondary stress systems are superposed. (1) Regional N–S compression was caused by convergence between the Iberian and African plates. (2) Multidirectional extension was caused by crustal doming in the Iberian Chain. (3) Stress trajectories were deflected near major faults. (4) Small-scale swapping of the horizontal tension axes (σ_2 and σ_3) was caused by development of fractures at right angles to either the primary or the deflected σ_3 axis.

INTRODUCTION

THE Iberian Chain and the Ebro Basin are situated in the northeast part of the Iberian Peninsula, and have undergone a parallel tectonic evolution during the whole of the Tertiary. The Iberian Chain is a NW–SE-trending intraplate fold-thrust belt formed mainly during the Palaeogene. The Ebro Basin is a foreland basin developed concomitantly along the northern margin of the Iberian Chain. During the Neogene both domains were affected by extension; two main stages can be distinguished (Miocene and Plio-Pleistocene), separated by the development of a major erosion surface over the whole of the Iberian Chain and Spanish Meseta. The Plio-Pleistocene extension deformed this surface and was responsible for the main morphotectonic features of the region. It constitutes the last tectonic event and is the major focus of this paper.

The large Pliocene and Quaternary structures in the region and their relationship with sedimentary and geomorphic processes are well known. However, there is a need for a dynamic model of the development of brittle structures at all scales. Modern methods of palaeostress analysis from striated faults measured in Neogene and Pleistocene deposits, as well as data on joint trends, are used to explore the mechanisms that determine the stress directions, their local deflection and relation to brittle structures. The final objective is a model of the Plio-Pleistocene stress field and fracturing in the Iberian Chain and Ebro Basin, in the context of the tectonic evolution of the eastern Iberian Peninsula.

SUMMARY OF THE NEOGENE–QUATERNARY EVOLUTION OF THE IBERIAN CHAIN AND EBRO BASIN

After the early–Middle Miocene, the N–S compression field created in the Iberian Chain and Ebro Basin as a result of the convergence between the Iberian and African plates interfered with E–ESE regional extension (Simón-Gómez & Paricio Cardona in press). As a consequence, a gradual transition between compression and extension regimes took place (Simón-Gómez 1986). The extension field was related to rifting along the eastern margin of the Iberian Peninsula and Valencia Basin. Rifting developed progressively from N to S (Vegas *et al.* 1979), so that the Iberian Chain underwent the stress change later than other regions of the Alpine Belt such as Languedoc, where extension began in the Middle–Upper Oligocene (Mattauer 1973), and the Catalan region (early Miocene, Cabrera Pérez 1981).

Two main episodes of Neogene extension were separated by a period of stability in which the *fundamental erosion surface* (Solé Sabarís 1978, Peña *et al.* 1984) developed. The first episode produced several grabens in the eastern Iberian Chain (Alfambra-Turia Graben, Maestrazgo Graben system) whose trend is parallel to the NNE axis of the rifting; this implies a dominant ESE extension which is also evident on a microstructural scale (Simón-Gómez 1984). The same direction of σ_3 has been found in the central Ebro Basin (Gracia Prieto & Simón-Gómez 1986); however, along the northern boundary of the Iberian Chain the σ_3 axis shows a NE–SW trend (Fontboté *et al.* 1985 unpublished abstract, Casas Sainz & Simón-Gómez 1986).

The second extensional episode deformed the fundamental erosion surface as well as the correlative deposits that had infilled the earlier grabens. The youngest of these deposits in the Alfambra-Turia Basin have been dated by microvertebrates as Upper Pliocene (Lower Villafranchian, biozone MN16, Moissenet 1983). The oldest clastic deposits appearing over the deformed surface also contain fauna of biozones MN16a (locality of Sarrión, Adrover 1986) or MN16b (localities of Concud and Gea, Moissenet 1983). Thus, the start of this second extensional phase is well established at the

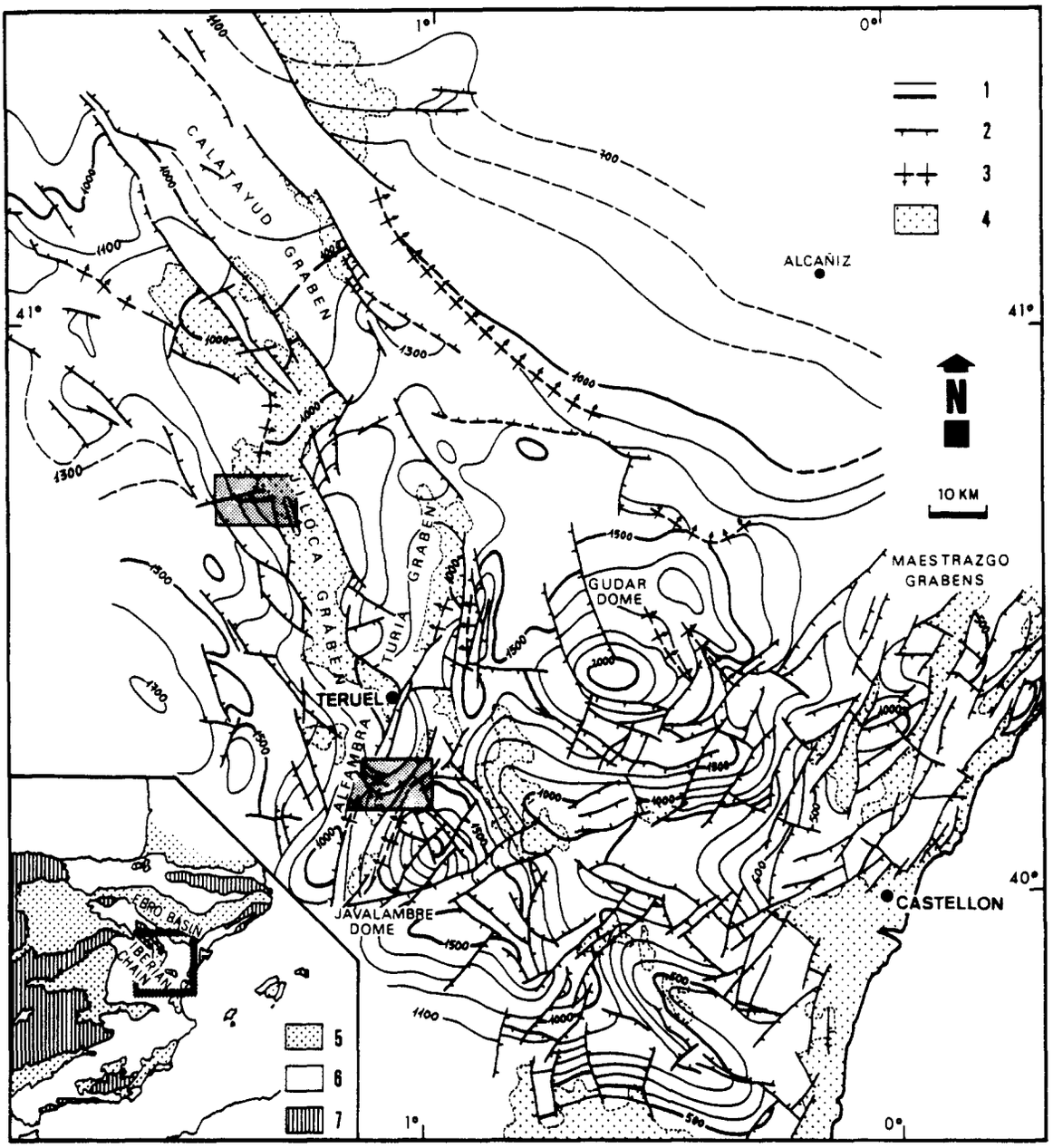

Fig. 1. Structural contour map of the deformed *fundamental erosion surface* (Upper Pliocene) in the central-eastern Iberian Chain. 1: Contours spaced at 100 m. 2 and 3: Faults and monoclines deforming the erosion surface. 4: Upper Pliocene–Quaternary deposits. Lower part: situation of the region within the Iberian peninsula. 5: Tertiary basins. 6: Mesozoic and Tertiary within Alpine Chains. 7: Palaeozoic. Contours in the area southwest of the Calatayud Graben are taken from Gracia Prieto *et al.* (1988).

beginning of the Upper Pliocene, around 3 Ma BP (Simón-Gómez 1984).

The *fundamental erosion surface* can be used as a marker surface in order to reconstruct the geometry of Plio-Quaternary structures. The contour map of the deformed surface in the central and eastern Iberian Chain (Fig. 1) displays a number of large faulted domes (Gúdar, Javalambre) and grabens (Calatayud, Jiloca, Alfambra-Turia, eastern Maestrazgo). Some of the grabens represent reactivation of others formed during the Miocene (Alfambra-Turia, Maestrazgo, Calatayud); the Ebro Basin also underwent renewed subsidence in the Pliocene. The only entirely new structure is the Jiloca Graben, which shows filling by sediments exclusively of Plio-Quaternary age.

Most of the structures expressed on the contour map of Fig. 1 probably formed during the period of greatest tectonic activity (Upper Pliocene). However, local deformation along the main faults also occurred during the early–Middle Pleistocene. Fracturing of this age has been reported along the Ebro Basin boundary (Gutiérrez *et al.* 1983), Jiloca and Alfambra-Turia Basins (Simón-Gómez 1983) and especially in the Maestrazgo Grabens, where displacements of almost 200 m have been documented (Simón-Gómez *et al.* 1983). Structures younger than the Middle Pleistocene are very rare; they are found almost exclusively along the eastern margin of the Jiloca Graben (Capote *et al.* 1981) and the top of the Javalambre Dome (Calvo Cases *et al.* 1983).

PLIO-PLEISTOCENE FRACTURING

Faults on the map scale

Major Plio-Pleistocene faults show a great variety of strikes (Fig. 1). However, if the complex fault pattern in the Javalambre and Gúdar domes is removed, two main directions of faults and graben axes are revealed: SSE and NNE. SSE is the direction of the graben originating from the Pliocene extension (Jiloca); the NNE direction, determined by the trend of the Mediterranean rifting, characterizes the grabens inherited from the Miocene extension (Alfambra-Turia and Maestrazgo).

In addition, several fault systems appear at right angles to the main graben faults. Two examples from the Jiloca Graben and the Alfambra-Turia Graben, respectively, are shown in Fig. 2. In both cases several E–W faults border or cut Upper Pliocene clastic deposits.

Fracturing on the outcrop scale

The analysis of map-scale faults does not permit reconstruction of the Plio-Pleistocene stress field, because of their inherited character and the difficulty in observing their planes and slip directions. Decimetre- to metre-scale fractures (faults and joints) observed in late Cenozoic deposits are more useful for this purpose. We distinguish faulting and jointing of (1) Upper Miocene–Lower Pliocene deposits (pretectonic in relation to the extension phase studied here) and (2) Upper Pliocene–Lower Pleistocene deposits (syntectonic).

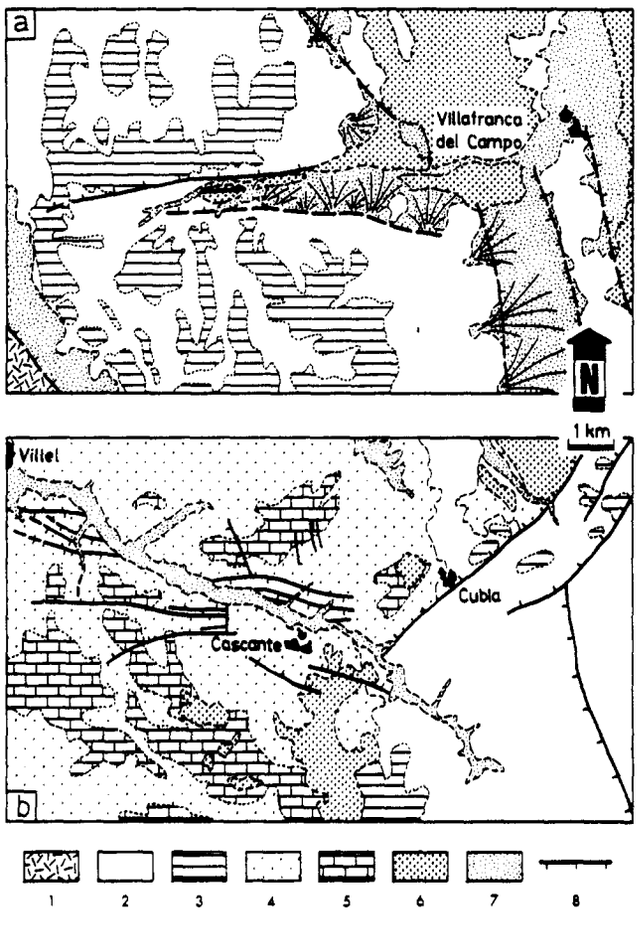

Fig. 2. Examples of macrofault sets orthogonal to graben boundaries. (a) Western margin of the Jiloca Graben. (b) Eastern margin of the Alfambra-Turia Graben (both areas are indicated in Fig. 1). 1: Palaeozoic. 2: Mesozoic. 3: *Fundamental erosion surface* on Mesozoic terrains. 4: Neogene. 5: Pliocene carbonate deposits correlated with the erosion surface. 6: Upper Pliocene clastic deposits. 7: Quaternary. 8: Plio-Quaternary faults.

Faults and joints in Upper Miocene–Lower Pliocene deposits

Directions of faults and joints observed in Mio-Pliocene deposits are shown in Fig. 3. Each small rosette diagram on the map represents about 50 joints or 25–35 normal faults measured at one station. Some strike-slip faults found at two of the sites have not been included in these diagrams. Each rosette of Fig. 3(b) represents a composite of data for each of the macrostructural domains in the region.

In spite of the diversity of joint and fault sets shown by the diagrams, some general characteristics seem to be evident:

In the *central Ebro Basin* there are two dominant orthogonal sets of faults and joints: one close to N–S and the other close to E–W.

Near the *boundary between the Ebro Basin and Iberian Chain* there are fractures parallel to the main faults of the basin edge (100–120° and 150°) and others roughly orthogonal (030–040°).

In the *Jiloca Graben* most of the fractures are oriented SE, although two sets can be differentiated: 160° and 120–130°; the first set is parallel to the graben axis; the second one is parallel to the major faults along its western boundary, which are clearly oblique to the graben trend. A less important set is also found around 020–040°.

In the *Alfambra-Turia Graben* the relation between micro and macrofaults is less clear. At stations 28 and 29 microfaults run parallel to the mapped faults ESE which are, themselves, orthogonal to the graben trend (see Fig. 2b). Other stations show an important set around 150° (Jiloca direction), whereas the NNE one is less well represented.

In the *Maestrazgo grabens* the main fracture direction is NNE, this is to say parallel to the macrofaults. An orthogonal set ESE (station 32) as well as the SSE/ENE pair (station 34) are also present.

Faults and joints in Upper Pliocene–Pleistocene deposits

The main fracture sets observed in Upper Pliocene clastic deposits are similar to those described above (Figs. 4a & b). One of the microfracture sets is usually parallel to the major young faults; a secondary orthogonal set is also common. The pair of SSE and ENE fracture sets is also present, in addition to the macrofault-controlled sets. In the Jiloca Graben, whose trend coincides with the SSE direction, fractures showing this strike prevail clearly.

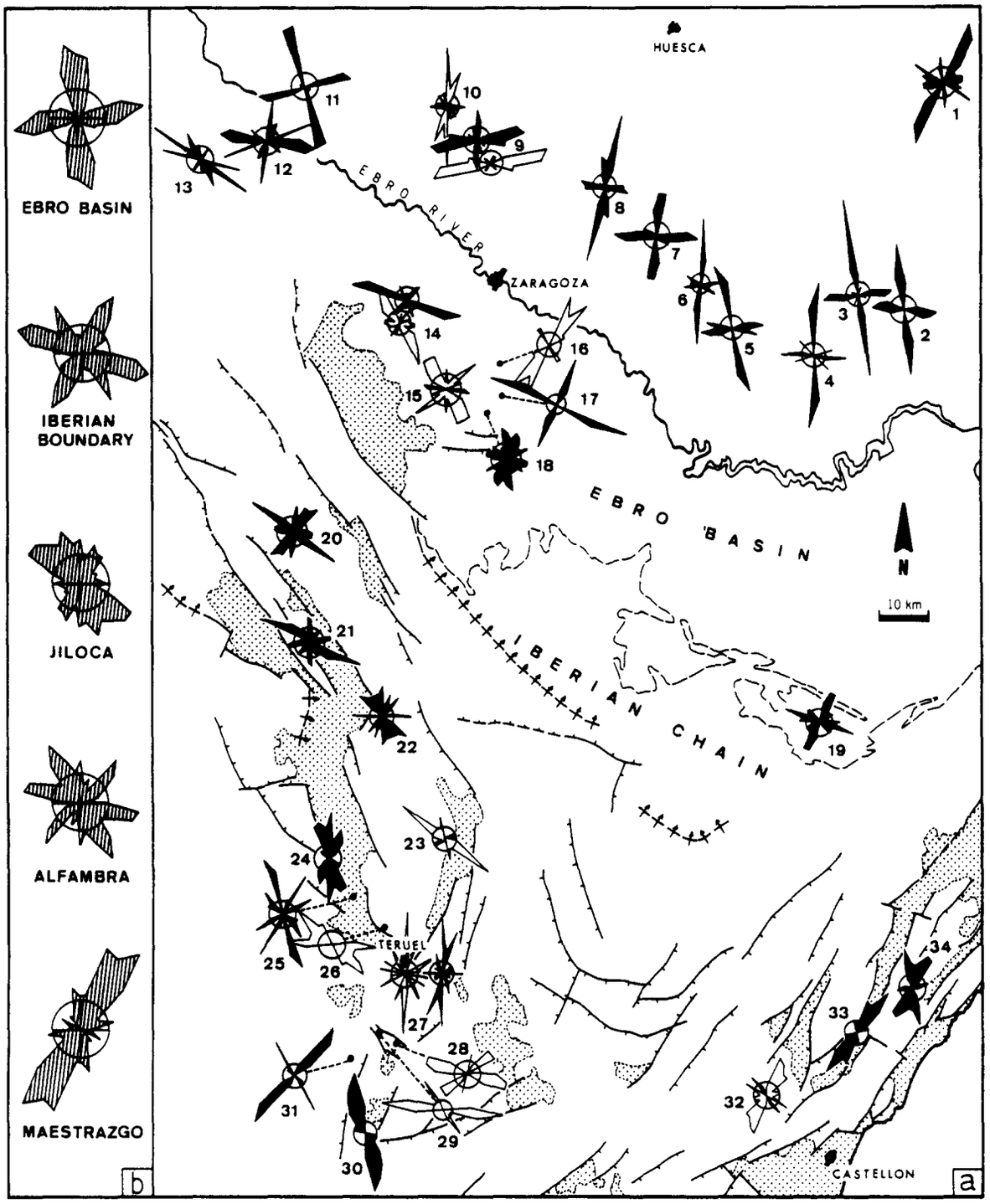

Fig. 3. Fracturing of Upper Miocene–Lower Miocene deposits. (a) Rosette diagrams for the analysed outcrops; black rosettes: joints; white rosette: faults. (b) Composite diagrams for the whole of the data for each macrostructural domain (Ebro Basin: stations 1–12; Iberian boundary: 13–19; Jiloca Graben: 20–22 and 24–26; Alfambra Graben: 23 and 27–31; Maestrazgo Grabens: 32–34). In all cases the diameter of the circle represents 5% of fractures for divisions of 10°.

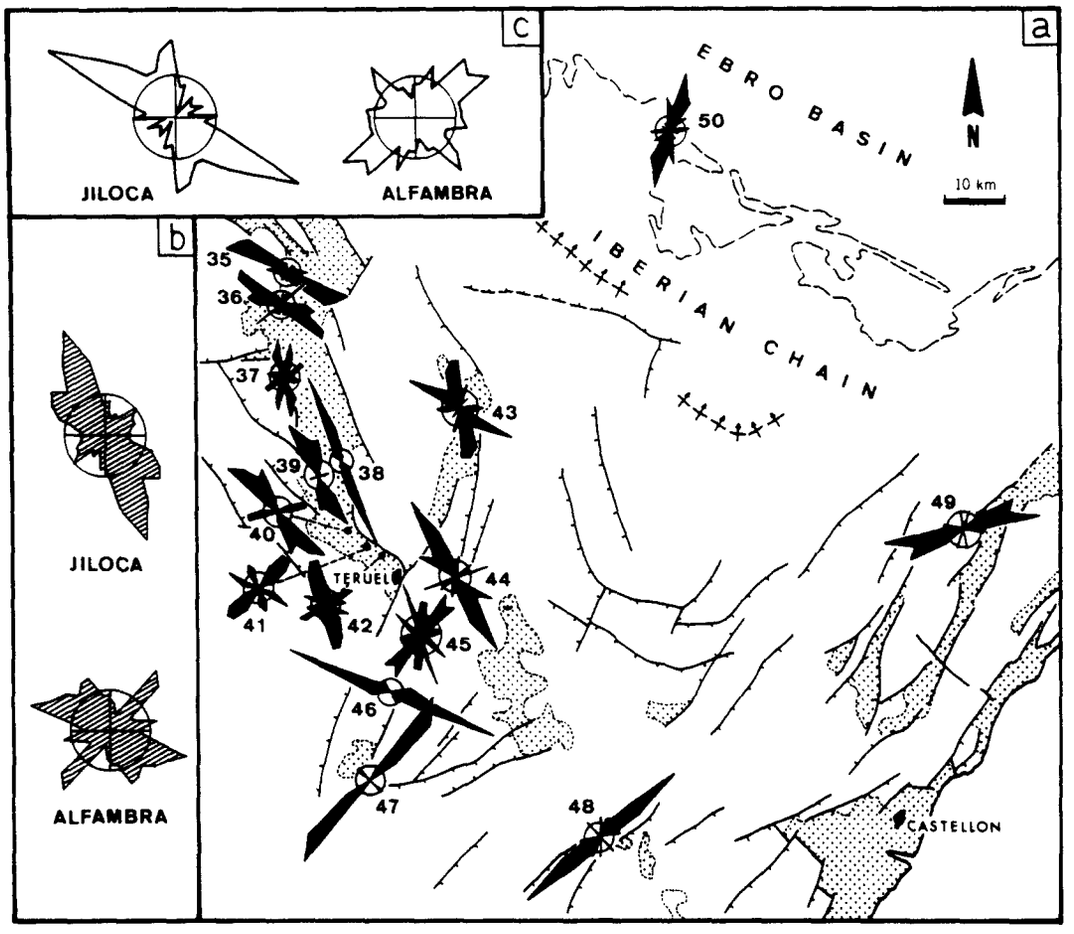

Fig. 4. (a) Rosette diagrams for fractures observed in Upper Pliocene deposits in the analysed outcrops. (b) Composite diagrams for all of the Upper Pliocene fractures measured in the Jiloca and Alfambra Grabens (stations 35–42 and 43–47, respectively). (c) The same diagrams for Pleistocene fractures. The diameter of circles corresponds to 5% of fractures for divisions of 10°.

Data on fracturing of Pleistocene deposits are less abundant, so that only two composite diagrams (Fig. 4c) are shown for all the data measured in the Jiloca and the Alfambra-Turia Grabens (118 and 104 fractures, respectively). A fairly clear concordance with fracture trends of the Upper Pliocene deposits can be noted.

PALAEOSTRESS ANALYSIS

Palaeostress analysis has been made from a total of 365 striated fault planes measured at 12 of the microstructural stations in Upper Miocene–Lower Pliocene deposits. In all cases the bedding surfaces are horizontal and only show minor displacement by faulting. Thus, the possibility that the faults have rotated during or after motion can be eliminated. Two methods are used for fault analysis whose combined application has proved to be very effective.

(1) *The numerical method of Etchecopar* et al. (1981)

This is a computer-aided iterative method applicable to multiphase fault populations which permits both separation and determination of successive deviatoric stress tensors. Solutions are identified as combinations of stress axis orientation and stress ratio $R = (\sigma_2 - \sigma_3)/(\sigma_1 - \sigma_3)$ which minimize the variance of angular deviations defined by $F = \Sigma\ (S_i,\ \tau_i)^2$ (S_i: striation; τ_i shear stress) for a given percentage of faults.

(2) *The* y–R *diagram* (*Simón-Gómez* 1986)

This is a graphical method in which one of the stress axes is considered to be vertical, so that only two variables are necessary to define the deviatoric stress tensor: y (azimuth of σ_y), and the stress ratio $R = (\sigma_z - \sigma_x)/(\sigma_y - \sigma_x)$, where σ_z is the vertical stress axis and $\sigma_y > \sigma_x$ are the horizontal axes. The infinite y–R combinations that can explain a single fault movement according to Bott's equation (Bott 1959) are represented by a curve on a two-co-ordinate diagram; the mean co-ordinates of 'knots' where a number of curves intersect represent optimum tensors.

General results of palaeostress analysis and several detailed examples are shown, respectively, in Figs. 5 and 6. Most of the stress ellipsoids show near vertical σ_1 axes and small R values, which implies a clear tendency towards radial or multidirectional tension ($\sigma_2 \simeq \sigma_3$). This tendency is more evident within the Ebro Basin; the average R ratio for stations 9, 10, 14, 15 and 16 is 0.05, and the σ_3 directions change greatly from point to point,

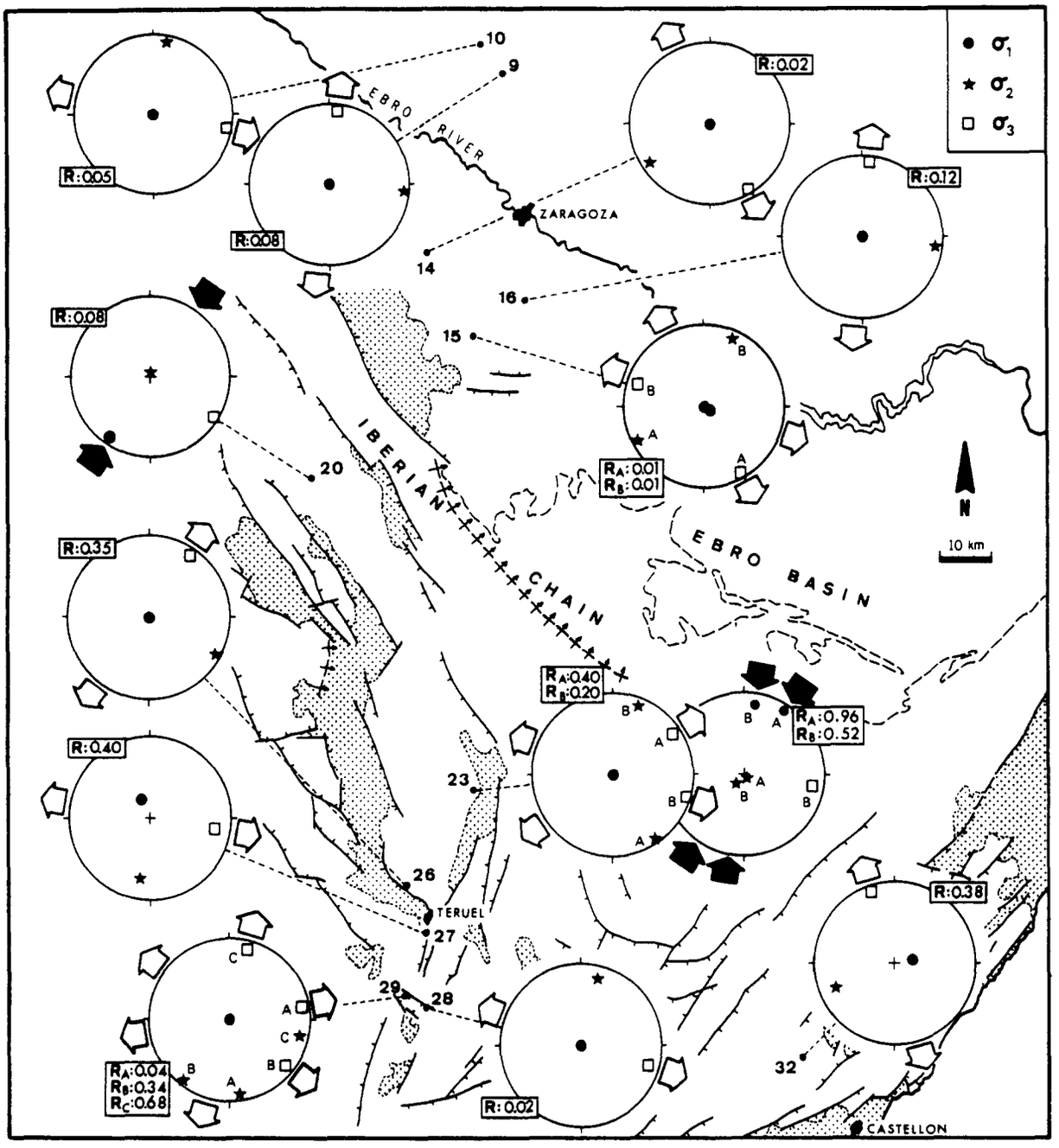

Fig. 5. Stress tensors inferred from fault striation analysis. $R = (\sigma_2 - \sigma_3)/(\sigma_1 - \sigma_3)$.

so that one may think that they have no meaning. However, most of the extension ellipsoids in the internal grabens of the Iberian Chain are triaxial (average $R = 0.31$), and the σ_3 directions tend to be orthogonal to the major faults (tensors 23B, 26, 27, 29C, 32) or parallel to them (tensors 28, 29B).

Almost all faults have a prevailing normal component, but conjugate sets roughly parallel to σ_2 with striation pitches close to 90° (e.g. Fig. 6a) are rare. On the contrary, faults oblique to σ_2 which show strike-slip components are common (e.g. Fig. 6b), as well as some cases in which the σ_3 axis of the optimum stress ellipsoid appears just parallel to the trend of the main microfault set (e.g. Fig. 6c).

Fig. 6. Results of palaeostress analysis from four types of fault populations using the methods of Etchecopar *et al.* (1981) and *y–R* diagram (Simón-Gómez 1986). (a) Concud (station 26). (b) Alcora (32). (c) La Muela (14). (d) Retascón (20). Fault planes and striae are represented in stereographic projection (Wulff net, lower-hemisphere) together with the orientations of the inferred stress axes (circle: σ_1; star: σ_2; square: σ_3), $R = (\sigma_2 - \sigma_3)/(\sigma_1 - \sigma_3)$. The histogram shows the distribution of angular deviations (in radians) between striation and shear stress on the analysed faults according to the inferred tensor. In the Mohr circle, planes corresponding to the explained faults are represented. The *y–R* diagram corroborates the former results and provides another different test for the quality of the solution. $R' = (\sigma_z - \sigma_x)/(\sigma_y - \sigma_x)$; y = azimuth of the major horizontal stress σ_y; if $R' > 1$, then $\sigma_y = \sigma_2$; if $R' < 1$, then $\sigma_y = \sigma_1$. The circle drawn on each plot indicates the region with the highest density of intersections. The location of this circle defines the optimum stress tensor, the diameter provides some idea about the confidence domain.

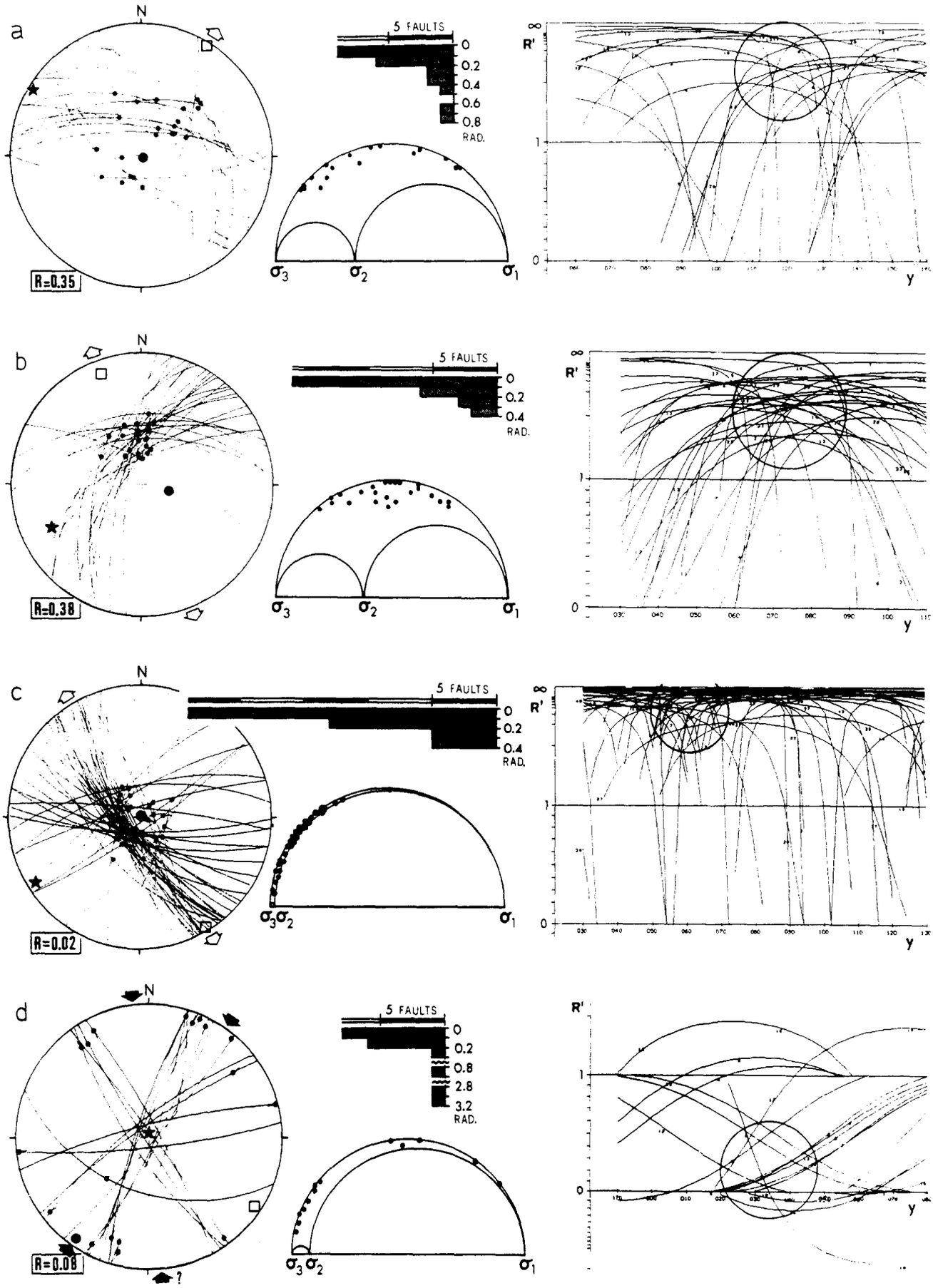
a
N
R=0.35
5 FAULTS
0
0.2
0.4
0.6
0.8
RAD.
σ3 σ2 σ1
R'
∞
1
0
y
b
N
R=0.38
5 FAULTS
0
0.2
0.4
RAD.
σ3 σ2 σ1
R'
∞
1
0
y
c
N
R=0.02
5 FAULTS
0
0.2
0.4
RAD.
σ3σ2 σ1
R'
∞
1
0
y
d
N
R=0.08
?
5 FAULTS
0
0.2
0.8
2.8
3.2
RAD.
σ3 σ2 σ1
R'
1
0
y

Fig. 6.

Some compressive stress tensors were also inferred from two strike-slip fault populations measured at stations 20 (Retascón, Zaragoza province) and 23 (Orrios, Teruel province). Results from the Etchecopar *et al.* and *y–R* methods applied to station 20 appear in Fig. 6(d). A good solution with σ_1 oriented 035°, 03° S, subvertical σ_2 and $R = 0.08$ (near uniaxial compression) explains 15 fault movements. Nevertheless, the geometry of faults suggests an initial conjugate system consistent with a σ_1 axis trending about 175°; in fact, two NNE fault planes showing right-lateral movement related to the main tensor also show left-lateral striations. In Orrios (station 23) a total of 58 normal, strike-slip and oblique fault movements have been measured. Most of them correspond to tensile states, but 19 strike-slip and oblique faults are explained by two compressive tensors: one has σ_1 033°, 04° N, subvertical σ_2 and $R = 0.96$ (it explains 11 faults); the other has σ_1 001°, 09° N, subvertical σ_2 and $R = 0.52$ (eight faults). Both ellipsoids are similar in orientation to those inferred at Retascón (station 20).

DISCUSSION

Results of palaeostress analysis, as well as fracture patterns and macrostructures (large domes and grabens along several trends), indicate that the dominant stress regime in the Iberian Chain and Ebro Basin during the Pliocene and Pleistocene was radial or multidirectional tension (vertical σ_1, $\sigma_2 \simeq \sigma_3$).

The extensional regime is probably due to crustal doming. Although little geophysical evidence exists, uparching of the crust in the central and eastern Iberian Chain during the Upper Pliocene, pushed up by a mantle diapir, is consistent with surface observations. One should remember that the region is close to the rift zone of the Valencia Basin; thus, doming and rifting must be related to each other within the geodynamic evolution of the eastern margin of the Iberian Peninsula during the Neogene.

Dome development might also be attributed to late isostatic movements. In fact, geophysical data seem to reveal a certain crustal thickening beneath the central-northern Iberian Chain (Vegas & Banda 1981, Zeyen *et al.* 1985). However, several facts suggest that, if present, isostatic uplift is not the main cause of vertical movements in the region:

(a) Doming took place mainly in the Upper Pliocene, long after folding in the chain had been completed, the two processes being separated by a period of relative stability.

(b) The geometry of the domes seems to be independent of the macrostructural trend of the chain or the geometry of crustal thickening; geophysical data show that the abnormally thin crust appearing beneath the Valencia Basin also extends into the southern part of the domed area (Zeyen *et al.* 1985).

(c) A number of large grabens are associated with domes, as well as with the rift system developed in the eastern margin of the Peninsula.

Doming can explain the multidirectional character of the Plio-Pleistocene extension field and, subsequently, the occurrence of orthogonal fault and joint systems and the influence that the major faults exert on the mesoscopic fractures. However, it is difficult to believe that all fractures form directly under the primary stress field. Models of *secondary or deflected stresses* in multidirectional extension fields proposed by Simón-Gómez *et al.* (in press) (based on mathematical simulation by the finite-element method and laboratory experiments) provide a more adequate explanation. These models suggest that secondary fractures appear (a) parallel and orthogonal to the primary σ_2 axis, and (b) parallel and orthogonal to the pre-existing discontinuities, as a consequence of two different stress redistribution phenomena.

(1) *Trajectory deflection caused by pre-existing faults.* The σ_3 trajectories become orthogonal near the ends and parallel in the centre. Faults reactivated below a cover show a tendency to propagate towards the surface, so that a set of fractures parallel to the main fault is induced in the overlying layer.

(2) *Swapping of the σ_2 and σ_3 axes,* caused by release of the primary normal tension.

The mathematical models also indicate an increase in the horizontal deviatoric stress ($\sigma_2 - \sigma_3$) around pre-existing faults, which can explain the difference between stress ratios obtained in the Ebro Basin, where major faults are absent, and those found in the internal grabens of the Iberian Chain.

Nevertheless, some of the fracture patterns found in the region cannot be explained only by doming. The constancy of a N–S trend of fracturing within the Ebro Basin suggests a primary tension field with preferred trajectories of σ_2 (around N–S) and σ_3 (around E–W), which probably become manifest when displacement on major faults is absent. In my opinion, the geometry of the domes does not justify these preferred trajectories, since no N–S elongated dome exists; this suggests the existence of another sort of tectonic mechanism able to produce anisotropy in horizontal tension. The orientation of the Jiloca Graben is another feature along the same lines; the only graben initiated under the Pliocene extension shows a precise SSE trend, different from that of the inherited grabens and oblique to its own faults (SE). This indicates the presence of relatively well-defined regional directions of σ_2 and σ_3 axes.

Tensors with horizontal compression trending N–NNE are also difficult to explain by doming. Some models of stress fields over domes have been proposed in which horizontal compression along radial trajectories is present, but always restricted to the dome periphery (Neugebauer 1978, Withjack 1979). In the case discussed here, compressive ellipsoids have been found inside the domed region, superposed on the tensile ellipsoids, and their orientations seem to be independent from the dome geometry.

In order to explain these 'anomalous' facts, the pres-

ent geodynamic setting of the Iberian Peninsula should be considered. The near N–S direction of both σ_2 axis of the primary tension field and σ_1 axis of the local compressive ellipsoids coincides with orientation of the Neogene–Quaternary regional compression in the southern margin of the Iberian plate, caused by the convergence with the African plate (Sanz de Galdeano 1983). This compressive field must extend into the Iberian plate, the magnitude of σ_1 becoming smaller northwards, which might determine a stress zonation similar to that proposed by Tapponier & Molnar (1976): triaxial compression (vertical σ_3) in the south of the Iberian Peninsula, strike-slip regime (vertical σ_2) in the centre (probably including the region studied here) and triaxial tension (vertical σ_1) in the north; the maximum horizontal axis (σ_1 or σ_2) is always oriented around N–S. However, radial tension induced by doming is superposed on the compression field and diminishes horizontal stresses. In most cases, σ_1 in the strike-slip zone becomes smaller than the vertical axis, with swapping of σ_1 and σ_2 taking place. Only at particular times, when doming rate diminishes or the horizontal compression increases, can compressive states be present.

In my opinion, the combination of the various primary and secondary stress systems postulated here allows the main features of the late Cenozoic brittle tectonics in the studied region to be explained. This model of a complex stress field is analogous to that proposed by Stauffer & Gendzwill (1987) for the Cenozoic evolution of a sector of North America (Saskatchewan, Montane and North Dakota), combining horizontal tensile stresses produced by vertical uplift and NE–SW compression due to plate motion.

CONCLUSIONS

Late Cenozoic brittle structures in the Iberian Chain and Ebro Basin developed within a complex tectonic setting. I propose a model of a stress field in which four components have been considered. Two are primary stress systems caused by two different geodynamic mechanisms which are superposed in the region:

(1) *N–S compression field* caused by the convergence between the Iberian and African plates. It extends over a great part of the Iberian Peninsula giving rise to local compressive states which have been documented in the Iberian Chain by means of small strike-slip and reverse faults.

(2) *Multidirectional tension field* caused by crustal doming in the Iberian Chain, related to the rifting in the Valencia Basin (eastern margin of the Iberian Peninsula). Superposition of this stress system on the compressive field gave rise to a decrease in the horizontal stresses and swapping of σ_1 and σ_2 axes. As a result, the primary stress field can be defined as nearly multidirectional tension with the σ_2 axis running approximately N–S. This is reflected by abundant N–S fracture sets (mainly in the central Ebro Basin) as well as by the macrostructural trend of the Jiloca Graben. At the same time large, nearly circular domes (Gúdar, Javalambre) developed, and several sets of pre-existing discontinuities were reactivated, including major faults along the edges of older grabens (Calatayud, Alfambra-Turia, Maestrazgo).

The other components of the model can be identified as stress redistribution phenomena:

(3) *Deflection of stress trajectories by major faults.* Trajectories of the σ_2 axis in the multidirectional tension field, and so the trends of secondary fractures, run either parallel or perpendicular to the major faults. Thus, in the grabens oriented NNE, sets of microfractures NNE and ESE occur, sometimes co-existing with S–SSE primary sets. In the Jiloca Graben, whose trend is roughly parallel to the primary σ_2 trajectories, the diversity of fracture sets decreases.

(4) *Small-scale swapping of the horizontal tension axes* (σ_2 *and* σ_3), caused by development of fractures within either the primary or the redistributed tension field. It provides a good explanation for the very common occurrence of orthogonal fracture systems, controlled by either the primary N–S field or the major faults.

Combining all these primary and secondary stress systems in different ways can explain adequately the late Cenozoic fracture patterns observed in the studied region. Difficulties easily arise as soon as we try to differentiate tectonic episodes within geodynamical environments where several tectonic mechanisms are superposed. In such cases, definition of *stress fields* (including primary components and internal secondary redistribution) provides a more realistic frame for the brittle tectonics development. The relationship between compression and tension during the Neogene–Quaternary in the eastern part of the Iberian Peninsula constitutes a typical problem that should be analysed in this perspective.

REFERENCES

Adrover, R. 1986. *Nuevas faunas de roedores en el Mio-Plioceno continental de la región de Teruel (España). Interés bioestratigráfico y paleoecológico.* Doct. thesis, Univ. Lyon I. Publ. Instituto de Estudios Turolenses, Teruel.

Bott, M. H. P. 1959. The mechanics of oblique slip faulting. *Geol. Mag.* **96**, 109–117.

Cabrera Pérez, L. 1981. Influencia de la tectónica en la sedimentación continental de la cuenca del Vallés-Penedés (provincia de Barcelona, España) durante el Mioceno inferior. *Acta geol. Hisp.* **16**, 165–171.

Calvo Cases, A., Gutiérrez Elorza, M., Peña Monné, J. L. & Simón-Gómez, J. L. 1983. Morfología de vertientes y neotectónica en el macizo de Javalambre (provincia de Teruel). *VI Reunión del Grupo Español de Trabajo del Cuaternario. Cuadernos del Laboratorio Xeoloxico de Laxe* **5**, 429–448.

Capote, R., Gutiérrez, M., Hernández, A. & Olivé, A. 1981. Movimientos recientes en la fosa del Jiloca (Cordillera Ibérica). *V Reunión del Grupo Español de Trabajo del Cuaternario,* Sevilla, 245–257.

Casas Sainz, A. & Simón-Gómez, J. L. 1986. Evolución del estado de esfuerzos durante la tectogénesis alpina en un sector del borde N de la Cordillera Ibérica (Alcaine, Teruel). *Estudios Geol.* **42**, 127–136.

Etchecopar, A., Vasseur, G. & Daignières, M. 1981. An inverse problem in microtectonics for the determination of stress tensors from fault population analysis. *J. Struct. Geol.* **3**, 51–65.

Gracia Prieto, F. J., Gutiérrez Elorza, M. & Leránoz Istúriz, B. 1988. Las superficies de erosión neógenas en el sector central de la Cordillera Ibérica. *Rev. Soc. geol. España* **1**, 135–142.

Gracia-Prieto, F. J. & Simón-Gómez, J. L. 1986. El campo de fallas miocenas de la Bardena Negra (provs. de Navarra y Zaragoza). *Boln Geol. Min.* **97**, 693–703.

Gutiérrez, M., Simón-Gómez, J. L. & Soriano, M. A. 1983. Tectónica cuaternaria en el área de la Almunia (prov. de Zaragoza). *VI Reunión del Grupo Español de Trabajo del Cuaternario, Cuadernos del Laboratorio Xeloxico de Laxe* **5**, 421–428.

Mattauer, M. 1973. *Les Déformations des Matériaux de l'Ecorce Terrestre.* Hermann, Paris.

Moissenet, E. 1983. Aspectos de la Neotectónica en la fosa de Teruel. In: *Geología de España. Libro Jubilar J.M. Ríos,* Vol. II (edited by Comba, J. A.). IGME, Madrid, 427–446.

Neugebauer, N. J. 1978. Crustal doming and the mechanism of rifting. Part I: rift formation. *Tectonophysics* **45**, 159–186.

Peña, J. L., Gutiérrez, M., Ibáñez, M. J., Lozano, M. V., Rodríguez, J., Sánchez, M., Simón-Gómez, J. L., Soriano, M. A. & Yetano, L. M. 1984. *Geomorfología de la provincia de Teruel.* Instituto de Estudios Turolenses, Teruel.

Sanz de Galdeano, C. 1983. La Neotectónica de las Cordilleras Béticas. In: *Geología de España. Libro Jubilar J.M. Rios,* Vol. II (edited by Comba, J. A.). IGME, Madrid, 469–485.

Simón-Gómez, J. L. 1983. Tectónica y neotectónica del sistema de fosas de Teruel. *Teruel* **69**, 21–97.

Simón-Gómez, J. L. 1984. *Compresión y distensión alpinas en la Cadena Ibérica oriental.* Doct. thesis, Univ. Zaragoza. Publ. Instituto de Estudios Turolenses, Teruel.

Simón-Gómez, J. L. 1986. Analysis of a gradual change in stress regime (example from the eastern Iberian Chain, Spain). *Tectonophysics* **124**, 37–53.

Simón-Gómez, J. L. & Paricio Cardona, J. In press. Sobre la compresión neógena en la Cordillera Ibérica. *Estudios Geol.*

Simón-Gómez, J. L., Pérez Cueva, A. & Calvo Cases., A. 1983. Morfogńesis y neotectónica en el sistema de fosas del Maestrat (provincia de Castellón). *Estudios Geol.* **39**, 167–177.

Simón-Gómez, J. L., Serón, F. J. & Casas, A. M. In press. Stress deflection and fracture development in a multidirectional extension regime. Mathematical and experimental approach with field examples. *Annales Tectonicæ.*

Solé Sabarís, L. 1978. La Meseta. In: *Geografía de España* (edited by De Terán, M.). Ariel, Madrid, 42–62.

Stauffer, M. R. & Gendzwill, J. 1987. Fractures in the northern plains, stream patterns and the midcontinent stress field. *Can. J. Earth Sci.* **24**, 1086–1097.

Tapponier, P. & Molnar, P. 1976. Slip-line field theory and large-scale continental tectonics. *Nature* **264**, 319–324.

Vegas, R. & Banda, E. 1981. Posible contribución de la Geofísica al conocimiento de la evolución geodinámica de la meseta ibérica (macizo Hespérico). *IV Asamblea Nacional de Geodesia y Geofísica,* Vol. I. IGME, Madrid, 389–396.

Vegas, R., Fontboté, J. M. & Banda, E. 1979. Widespread neogene rifting superimposed on alpine regions of the Iberian peninsula. *Proceedings Symp. Evolution and Tectonics of the Western Mediterranean and Surrounding areas. Spec. Publs Instituto Geográfico Nacional, Madrid* **201**, 109–128.

Withjack, M. 1979. An analytical model of continental rift fault patterns. *Tectonophysics* **59**, 59–81.

Zeyen, H. J., Banda, E., Gallart, J. & Ansorge, J. 1985. A wide angle seismic reconnaissance survey of the crust and upper mantle in the Celtiberian Chain of eastern Spain. *Earth Planet. Sci. Lett.* **75**, 393–402.